


# Molecular dynamics evaluation of self-diffusion coefficients in two-dimensional dusty plasmas

Muhammad Asif Shakoori, Misbah Khan, Haipeng Li(李海鹏), Aamir Shahzad, Maogang He(何茂刚), and Syed Ali Raza

**Citation:** Chin. Phys. B, 2025, 34 (**4**): 045202. DOI: 10.1088/1674-1056/adacce
Journal homepage: http://cpb.iphy.ac.cn; http://iopscience.iop.org/cpb

**What follows is a list of articles you may be interested in**

---

## Shear rheology of confined double rings of dust particles in a dusty plasma

Miao Tian(田淼), Jiaqi Li(李佳琪), Xuebo Yu(于雪波), Xue Liu(刘雪), Shaopeng Li(李绍鹏), Qing Li(李庆), Fucheng Liu(刘富成), and Yafeng He(贺亚峰)

Chin. Phys. B, 2024, 33 (**12**): 125201. DOI: 10.1088/1674-1056/ad8552

## Global dust density in two-dimensional complex plasma

Yi-Zhen Zhao(赵逸真), Song-Fen Liu(刘松芬), Wei Kong(孔伟), and Fang Yang(杨芳)

Chin. Phys. B, 2024, 33 (**6**): 065201. DOI: 10.1088/1674-1056/ad2a76

## Differences between two methods to derive a nonlinear Schrödinger equation and their application scopes

Yu-Xi Chen(陈羽西), Heng Zhang(张恒), and Wen-Shan Duan(段文山)

Chin. Phys. B, 2024, 33 (**2**): 025203. DOI: 10.1088/1674-1056/ad082b

## Long-time evolution of charged grains in plasma under harmonic external force and after being withdrawn

Miao Guan(管苗), Zhi-Dong Chen(陈志东), Meng-Die Li(李梦蝶), Zhong-Mao Liu(刘忠茂), You-Mei Wang(汪友梅), and Ming-Yang Yu(郁明阳)

Chin. Phys. B, 2022, 31 (**2**): 025201. DOI: 10.1088/1674-1056/ac0e27

## Crystalline order and disorder in dusty plasmas investigated by nonequilibrium molecular dynamics simulations

Aamir Shahzad, Maogang He, Sheeba Ghani, Muhammad Kashif, Tariq Munir, Fang Yang

Chin. Phys. B, 2019, 28 (**5**): 055201. DOI: 10.1088/1674-1056/28/5/055201

---

# Molecular dynamics evaluation of self-diffusion coefficients in two-dimensional dusty plasmas

Muhammad Asif Shakoori[1,†], Misbah Khan[2], Haipeng Li(李海鹏)[1,‡], Aamir Shahzad[3], Maogang He(何茂刚)[4], and Syed Ali Raza[5]

[1] *School of Materials Science and Physics, China University of Mining and Technology, Xuzhou* 221116, *China*
[2] *Department of Refrigeration and Cryogenic Engineering, School of Energy and Power Engineering, Xi'an Jiaotong University, Xi'an* 710049, *China*
[3] *Department of Physics, Government College University Faisalabad (GCUF), Allama Iqbal Road, Faisalabad* 38000, *Pakistan*
[4] *Key Laboratory of Thermo-Fluid Science and Engineering of Ministry of Education (MOE), Xi'an Jiaotong University, Xi'an* 710049, *China*
[5] *School of Electrical Engineering, Xi'an Jiaotong University, Xi'an* 710049, *China*

(Received 25 November 2024; revised manuscript received 13 January 2025; accepted manuscript online 22 January 2025)

We employ the Green–Kubo (G-K) and Einstein relations to estimate the self-diffusion coefficients (denoted as $D_{\rm G}$ and $D_{\rm E}$, respectively) in two-dimensional (2D) strongly coupled dusty plasmas (SC-DPs) via equilibrium molecular dynamics (EMD) simulations. $D_{\rm G}$ and $D_{\rm E}$ are computed for a broad domain of screening length ($\kappa$) and coupling parameters ($\Gamma$) along with different system sizes. It is observed that both $D_{\rm G}$ and $D_{\rm E}$ decrease linearly with increasing $\Gamma$ in warm liquid states and increase with increasing $\kappa$. In cold liquid states, the Einstein relation accurately predicts $D_{\rm E}$ in 2D SC-DPs because diffusion motion is close to normal diffusion, but the G-K relation provides overestimations of $D_{\rm G}$, because VACF indicates anomalous diffusion; thus, $D_{\rm G}$ is not accurate. Our new simulation outcomes reveal that $D_{\rm G}$ and $D_{\rm E}$ remain independent of system sizes. Furthermore, our investigations demonstrate that at higher temperatures, $D_{\rm G}$ and $D_{\rm E}$ converge, suggesting diffusion motion close to normal diffusion, while at lower temperatures, these two values diverge. We find reasonable agreement by comparing current and existing numerical, theoretical and experimental data. Moreover, when normalizing diffusion coefficients by the Einstein frequency and testing against the universal temperature scaling law, $D_{\rm G}$ deviates from theoretical curves at low temperatures and $\kappa$, whereas $D_{\rm E}$ only disagrees with theory at very small $\kappa$ ($\simeq 0.10$). These findings provide valuable insight into diagnosing dust component parameters within 2D DP systems and contribute to the broader understanding of diffusion processes in DP environments.

**Keywords:** dusty (complex) plasmas, self-diffusion coefficients, molecular dynamics simulation, Green–Kubo and Einstein relations

**PACS:** 52.27.Lw, 52.65.Yy, 66.10.Cg

**DOI:** 10.1088/1674-1056/adacce **CSTR:** 32038.14.CPB.adacce

## 1. Introduction

Dusty plasmas (DPs) are an ideal test system for the study of numerous physical phenomena in strongly coupled systems due to the macroscopic size of the dust particles and the experimentally achievable high coupling strengths.[1] Notable examples include the Wigner lattice of electrons on the surface of liquid helium,[2] arrays of vortices in the dynamic He mixed state type-II superconductors,[3] colloidal suspensions,[4] ions confined in penning traps,[5] DPs[6,7] and Brownian motion in particle systems on water surfaces.[8] Among these, two-dimensional (2D) DPs liquids have garnered significant interest due to their unique properties arising from interparticle interactions within a plasma background. Understanding mass transport, specifically diffusion in these DP systems, is vital for theory, simulation and experiments in various fields, such as plasma physics, semiconductor and chemical industries, polymer physics, nuclear energy generation, environmental and space sciences, dense stars, planetary interiors, highly ionized gases and plasma-based material processing. Recent reviews have focused on physics and applications from different perspectives of DPs.[9] The understanding and estimation of transport processes in DPs hold particular relevance for advancing micro and nano technologies. The investigation of dust transport processes, with or without external forces, poses a fundamental challenge in statistical mechanics.[9]

Self-diffusion refers to the process by which dust particles spread out over time due to random thermal motion or interaction. It plays a significant role in different disciplines of science and technology. For example, fluid mechanics, material science, nanotechnology, particle physics, biophysics, etc. Knowledge of self-diffusion of 2D DPs is essential in the disciplines of fundamental plasma physics, astrophysics, design of DP devices and dust particle charging and coagulation. Overall, the diffusion of dust particles helps to determine the energy dissipation (stopping power), characterizes dynamics as waves and instabilities, and modi-

†Corresponding author. E-mail: asif-shakoori@cumt.edu.cn
‡Corresponding author. E-mail: haipli@cumt.edu.cn

© 2025 Chinese Physical Society and IOP Publishing Ltd. All rights, including for text and data mining, AI training, and similar technologies, are reserved.

fies the phase transition, vortices and heating processes.[10–15] The diffusion behavior of dust particles in a plasma background is generally investigated using the standard Green–Kubo (G-K) and Einstein relations.[16] From the G-K relation, the self-diffusion motion is characterized by velocity autocorrelation function (VACF), coefficients ($D_{\rm G}$), and using the Einstein relation, motion through mean square displacement (MSD) and coefficients ($D_{\rm E}$). Both the G-K and Einstein relations were extensively used in different simulation techniques such as molecular dynamics (MD),[16–18] Langevin molecular dynamics (LMD)[13–15] and Brownian molecular dynamics (BMD)[12,19] simulations. These relations give similar results from simulation and experimental results and validate different effective potential and kinetic theories.[20–22]

While providing the literature on self-diffusion in DPs, we focused only on the investigations of VACF, MSD, $D_{\rm G}$ and $D_{\rm E}$ for three-dimensional (3D) and 2D DPs obtained through simulation techniques such as MD,[16,18,23–32] LMD[13–15] and BMD simulations,[12,19] theories[20–22] and experiments.[10,33] To the best of our knowledge, the MD simulation had been carried out for 3D one-component plasmas (OCPs) and the data of VACF and $D_{\rm G}$ in 3D reported for the first time by Vieillefosse *et al.*,[25] and MSD and $D_{\rm E}$ by Robbins *et al.*[34] over a wide domain of plasma parameters. Lowen *et al.*[19] performed the MD and BMD simulation techniques and reported results of VACF and $D_{\rm G}$ in 3D Yukawa fluid near the melting point. Rosenfeld *et al.*[35] reported reduced $D_{\rm G}$ through MD simulation in 3D OCPs. Ohta and Hamaguchi[16] published the MD results of VACF, MSD, $D_{\rm G}$ and $D_{\rm E}$ in 3D DPs for a wide range of plasma Debye screening strength ($\kappa = 0.1$–$5.0$) and Coulomb coupling ($\Gamma = 0.987$–$12300$).

In addition, Daligault implemented MD simulations and investigated the VACF and $D_{\rm G}$ in 3D weakly coupled (WC) to strongly coupled (SC) regimes of OCPs ($\kappa = 0$) as well in DPs ($\kappa = 1$–$4$),[36] and in ionic mixtures for intermediate to a higher number of particles.[17] Next, He[26] reported $D_{\rm G}$ over a wide range of inverse screening strength versus an entire range of coupling parameters. Vaulina *et al.* investigated $D_{\rm E}$ in 3D SC-DPs through the BMD[12] and the LMD[13] methods. Furthermore, they employed the LMD method and reported $D_{\rm E}$ in 2D DPs ($\Gamma^* = 1.5$–$225$, $\kappa < 6$), and the results were compared with 3D systems.[14] Next, they reported the VACF, $D_{\rm G}$, MSD and $D_{\rm E}$ in 2D ($\Gamma^* = 1.5$–$225$) and 3D systems over a wide range of parameters.[15] Liu *et al.*[37] estimated the VACF and MSD using MD simulation to point out defects in 2D DPs. Liu and Goree investigated the diffusion in 2D DPs from different perspectives. For example, they identified the region where Stokes–Einstein relation is applicable,[38] indicating the superdiffusion at intermediate temperature through three tests (MSD, probability distribution function and VACF),[39] experimentally detecting superdiffusion using the MSD test[40,41] and simulation (MD),[40] and investigating the force and energy dependence perpendicular diffusion coefficients in SC-DPs using LMD simulation.[42] Hou *et al.*[43] used BMD simulation for 2D SC-DPs and investigated self-diffusion (MSD and VACF). They observed a transition from superdiffusion to normal diffusion, then subdiffusion with increasing damping rates. Donko *et al.*[44] computed self-diffusion (VACF and MSD) in 2D SC-DPs using MD simulation. Shahzad and HE reported the EMD simulation data of VACF and MSD in 2D SC-DPs[45] and WC-DPs.[46] Ghannad and Pajouh[47] studied the memory effects in velocity processes to compute the MSD and VACF in DPs. They concluded that the presence of memory effects in the velocity process induced anomalous diffusion in DPs. Ghannad reported non-Guassian diffusion[48] and identified the time scale of the violation of the Stokes–Einstein relation.[49] Kostadinova *et al.*[50] analytically investigated anomalous diffusion in 2D DPs. Sheridan[51] investigated self-diffusion in 2D DPs. Wang *et al.*[52] reported the anomalous diffusion of charged dust particles in the plateau regime of toroidal plasma. Charan *et al.*[53] reported MD studies on $D_{\rm G}$ and $D_{\rm E}$ ($\Gamma = 150$, $\kappa = 2$) diffusion in the presence and absence of gravitational force.

Baalrud and Daligault provided the effective potential,[20] modified Enskog kinetic theory,[21] and provided a practical model[26] for the transport process in WC-SC regimes of DPs. Daligault[26] also calculated $D_{\rm G}$ using MD simulations, and obtained results that compared well with different effective potential[20] and kinetic theories.[21] They concluded that MD data of $D_{\rm G}$ are well matched with different kinetic theories and effective potentials of 3D WC-SC regimes of OCPs. Losseva *et al.*[54] proposed a self-consistent model to account for the ambipolar diffusion of ions and electrons in DPs. Gabdulin *et al.*[55] studied sound speed in 2D SC-DPs by calculating the VACF through MD simulation. Nunomura *et al.*[10] reported experiments to investigate the MSD and $D_{\rm E}$ in 2D DPs. Then, Strickler *et al.*[33] experimentally measured the VACF and $D_{\rm G}$ in 3D ultracold neutral plasma and compared their estimated values of diffusion coefficients with MD outcomes.[17,26] These comparisons show that the MD outcome of diffusion coefficients using the G-K and Einstein relations yields nearly similar results, with experimental values obtained from the Einstein relation being nearly similar to the MD outcomes. Shakoori *et al.*[18] investigated $D_{\rm E}$ for 3D DPs and reported that $D_{\rm E}$ is independent of different system sizes. Their comparisons with Refs. [16,17,26] show excellent agreement.

The above literature indicates that both the G-K and Einstein relations have been extensively employed in numerous simulation methods and experimental studies to analyze the self-diffusion of dust particles in DPs. Self-diffusion in 3D DP

systems is extensively reported. However, there is limited literature on the 2D case. To the best of our knowledge, Vaulina *et al.* used the LMD simulation method to investigate $D_{\rm E}$[14] and $D_{\rm E}$ and $D_{\rm G}$[15] ($\Gamma^* \approx 1.5$–225, $\kappa < 6$). Nunomura *et al.*[10] reported MSD and $D_{\rm E}$ [$T \approx 20$, 40 (eV)] experimentally in 2D DPs and compared their findings with the MD outcomes of 3D OCPs.[23,25,34] Hartmann *et al.*[11] reported $D_{\rm E}$ in magnetized and unmagnetized 2D DPs through experimental and simulation (MD) methods ($\Gamma^* \approx 20$–125, $\kappa = 1.0$). A comprehensive study of the diffusion coefficients ($D_{\rm G}$ and $D_{\rm E}$) in 2D complex plasmas (DPs) across a broad range of plasma parameters ($\Gamma = 1$–1100, $\kappa = 0.10$–3) and system sizes ($N = 400$–10000) has not been conducted. This highlights a significant gap in the current literature concerning the detailed investigation of diffusion behavior in 2D DPs under varying conditions. This lack of research served as our motivation to conduct a comprehensive investigation into the MD evaluation of $D_{\rm G}$ and $D_{\rm E}$ in 2D DPs and compare current outcomes with previous 3D simulations and experimental data.

The purpose of this study is to investigate $D_{\rm G}$ and $D_{\rm E}$ in 2D DPs through MD simulation by employing the G-K and the Einstein relations and subsequently comparing and analyzing the results. In Section 2, we describe the MD simulation technique for 2D DPs and the G-K and the Einstein relations to obtain $D_{\rm G}$ and $D_{\rm E}$. In Section 3, we present and discuss the calculated $D_{\rm G}$ and $D_{\rm E}$ by comparing them with previous numerical and experimental data. In Section 4, we provide the conclusion of this study.

## 2. Molecular dynamics simulation method

The process of MD simulation has proved to be a valuable tool for studying DPs at the microscopic level. In this technique, the dust particles and the surrounding plasma are treated as individual entities that interact according to specific interatomic or intermolecular potentials.[7,56] The most crucial part is selecting the interaction potential while implementing the MD simulations. The Yukawa potential is frequently used to calculate the interaction and forces between the dust particles in the plasma medium. It can be employed in other physical systems such as the physics of chemicals and polymers, medicine, biology, astrophysics, environmental science, etc. Notably, one of the key advantages of employing the Yukawa potential is its ability to reduce calculation time compared to other potentials.[7] The interaction energy of a charged particle in plasmas can be written as

$$\phi(r_{ij}) = \frac{Q^2}{4\pi\varepsilon_0}\frac{\exp\frac{-r_{ij}}{\lambda_{\rm D}}}{|r_{ij}|}, \tag{1}$$

where $Q$ represents the charge magnitude, $r_{ij}$ denotes the interparticle distance between the two dust particles, $\lambda_{\rm D}$ is the Debye length and $\varepsilon_0$ represents the permittivity of free space. The Newtonian equation of motion can be implemented to calculate the trajectories of $N$ particles in both 2D and 3D systems. The force on each dust particle is determined from negative derivatives of Yukawa potential as $F_{ij} = -\partial\phi(r_{ij})/\partial r_{ij}$. The DPs are characterized by two dimensionless parameters; the coupling parameter (Coulomb systems) is defined as

$$\Gamma = \frac{Q^2}{4\pi\varepsilon_0}\frac{1}{a_{\rm ws}k_{\rm B}T}. \tag{2}$$

The parameters described in Eq. (2) include the Wigner–Seitz radius ($a_{\rm ws}$) defined as $(2n\pi)^{\frac{-1}{2}}$ for a 2D system, where $n = N/A$ represents the equilibrium dust number density, $A$ is the area of the simulation box, $k_{\rm B}$ denotes the Boltzmann constant and $T$ signifies system temperature. The parameter $\Gamma$ measures the ratio of average potential energy to kinetic energy among interacting dust particles in plasma. The classification of DPs into SC and WC systems is determined by $\Gamma$, where SC-DPs are associated with $\Gamma > 1$, while WC-DPs with $\Gamma < 1$.[7,44] The second dimensionless parameter, $\kappa$, can be defined as $\kappa = a_{\rm ws}/\lambda_{\rm D}$, $\kappa \approx 0$ for the case of OCPs (Coulomb systems with crystallization limit, $\Gamma_{\rm m} \approx 137$) and $\kappa \approx \infty$ (hard-sphere interaction).[34] The plasma frequency for 2D DPs can be written as $\omega_{\rm p} = (nQ^2/(2\varepsilon_0 m a_{\rm ws}))^{\frac{-1}{2}}$.

### 2.1. Green–Kubo relation for self-diffusion coefficients

The G-K and Einstein relations are usually used to compute the self-diffusion of particles in gas, liquid and materials. These methods need time series calculations for the positions and velocities of particles. The self-diffusion of dust particles can be investigated with the help of the standard MD simulation method by employing the G-K and the Einstein relations. The G-K method is commonly used to calculate transport properties such as shear viscosity,[30] thermal conductivity[7] and self-diffusion[18] of DPs and simple liquids. The G-K relation measures $D_{\rm G}$ for the relevant hydrodynamic fluxes and time correlation function. It should be noted here that the G-K relation for $D_{\rm G}$ has been extensively used in numerous numerical methods,[16–18,25] and experimental studies[33] can be written for 2D systems as

$$D_{\rm G}(t) = \frac{1}{2N}\sum_{j=1}^{N}\int_0^{\infty}\langle v_j(t)\cdot v_j(0)\rangle {\rm d}t, \tag{3}$$

where $N$ is the number of simulated particles and $\langle v_j(t)\cdot v_j(0)\rangle$ is known as VACF. The VACF, which has been employed in studies of diffusion for 3D DPs[16] as well as for 2D DP systems of SC-DPs and WC-DPs[18,44,45] demonstrated its broad applicability and accuracy and is adopted in the present study as well.

### 2.2. Einstein relation for self-diffusion coefficients

The second relation used to investigate self-diffusion is Einstein; in this method, the motion of particles is analyzed from the slope of MSD in the long time limit and can also obtain the diffusion coefficients[14,16] as

$$D_{\mathrm{E}}(t) = \lim_{t\to\infty} \frac{1}{4t} \langle |\boldsymbol{r}_j(t) - \boldsymbol{r}_j(0)|^2 \rangle, \tag{4}$$

where $\boldsymbol{r}_j$ represents the position vector of $j$th particles and $\langle |\boldsymbol{r}_j(t) - \boldsymbol{r}_j(0)|^2 \rangle$ is known as MSD. Equation (4) was previously used to compute $D_{\mathrm{E}}$ in 3D,[16,18] 2D DPs[15,38] and in experiments.[10] $D_{\mathrm{G}}(t)$ and $D_{\mathrm{E}}(t)$ as $t \to \infty$, both tend to a constant value, which is the definition of diffusion coefficients. The angular brackets $\langle \cdots \rangle$ in Eqs. (3) and (4) represent canonical ensembles, take the average of all particles, and theoretically give the same values of $D_{\mathrm{G}}$ and $D_{\mathrm{E}}$ at the same parameters.[15,16]

### 2.3. EMD simulation parameters

The EMD simulations code (developed by the authors[18,30,45,46]) has been used for 2D SC-DPs to compute the $D_{\mathrm{G}}$ and $D_{\mathrm{E}}$ in microcanonical ensembles (NVE). In this study, we employed a 2D orthorhombic box geometry with standard periodic boundary conditions (PBCs) to model DP systems consisting of $N = 400$, 4096 and 10000 dust particles in a plasma background. The simulation box is defined by two orthogonal axes, $x$ and $y$, each of which can have its distinct normalized length as $L_x a_{\mathrm{ws}} \neq L_y a_{\mathrm{ws}}$, allowing for flexibility in simulating systems. The PBCs ensure that particles exiting one side of the box re-enter from the opposite side, effectively creating an infinite, repeating system that eliminates artificial boundary effects. This setup allows the system to approximate bulk behavior, particularly in the study of long-range interparticle interactions. Moreover, the orthorhombic geometry's capacity to accommodate different aspect ratios provides the flexibility to model 2D DPs, while maintaining computational efficiency. This approach is particularly well-suited to investigating diffusion coefficients.[57] Yukawa potential [Eq. (1)] is used to compute the interactions between dust particles,[7] and the long-range interactions between the dust particles are calculated using the Ewald summation method with the appropriate Ewald convergence parameter ($= 5.6$) for relative accuracy.[58] Newton's equation of motion is integrated with the leap-frog integration algorithm[56] for using $N$ particles to calculate each particle's position, force and acceleration with the appropriate simulation time step ($\mathrm{d}t = 0.001/\omega_{\mathrm{p}}$). Appropriate input parameters are selected to ensure the accuracy of the used EMD simulation scheme. These parameters, including the system temperature ($T = 1/\Gamma$), screening length, total number of particles, time step for each calculation, run time, etc, are used to obtain $D_{\mathrm{G}}$ and $D_{\mathrm{E}}$ in 2D SC-DPs. The MD simulations were run up to $\omega_{\mathrm{p}}t = 200$ for $\kappa = 0.1$ to 1.0, ensuring the system reached equilibrium. For $\kappa = 2$ and 3, the condition $t_{\mathrm{obs}} < a_{\mathrm{ws}}(N\pi)^{\frac{1}{2}}/c$ was followed, with simulations extending up to $\omega_{\mathrm{p}}t = 800$,[44,59] to allow sound waves to enter the simulation box and calculate $D_{\mathrm{G}}$ using the G-K relation. For the Einstein relation, the simulation was run long enough ($\omega_{\mathrm{p}}t = 3000$) and $D_{\mathrm{E}}$ was obtained at a fixed time for all parameters, and this long time may satisfy the $\mathrm{MSD}(t) > N a_{\mathrm{ws}}^2$.[11] In this paper, the EMD simulation technique is used to produce the plasma $D_{\mathrm{G}}(\Gamma, \kappa)$ and $D_{\mathrm{E}}(\Gamma, \kappa)$ for the entire range of coupling ($1 \leq \Gamma \leq 1100$) and screening length ($0.10 \leq \kappa \leq 3$) by simulating three different system sizes ($N = 400$, 4096 and 10000).

## 3. Results and discussion

In this subsection, we report the calculated values of self-diffusion coefficients in 2D SC-DPs using EMD simulations for a wide range of plasma parameters ($\Gamma$, $\kappa$) along with different $N$. The effects of plasma $\Gamma$, $\kappa$ parameters and $N$ on $D_{\mathrm{G}}(\Gamma, N, \kappa)$ and $D_{\mathrm{E}}(\Gamma, N, \kappa)$ in 2D SC-DPs have been analyzed and discussed. $D_{\mathrm{G}}$ and $D_{\mathrm{E}}$ reported in this study are normalized by plasma frequency as $D_{\mathrm{G}}^0 = D_{\mathrm{G}}/(\omega_{\mathrm{p}} a_{\mathrm{ws}}^2)$ and $D_{\mathrm{E}}^0 = D_{\mathrm{E}}/(\omega_{\mathrm{p}} a_{\mathrm{ws}}^2)$. The major results are displayed in Figs. 1–5, where we calculate $D_{\mathrm{G}}^0(\Gamma^*, N, \kappa)$ and $D_{\mathrm{E}}^0(\Gamma^*, N, \kappa)$ through EMD simulations in 2D SC-DPs. It should be noted here that the log–log scale is implemented in Figs. 1–9, for clarity and fair comparison. These results are calculated for a broad domain of plasma coupling ($\Gamma = 1$, 2, 3, 5, 10, 20, 50, 100, 200, 300, 500, 700, 900 and 1100) by simulating different system sizes ($N = 400$, 4096 and 10000) for each plasma screening length ($\kappa = 0.1$, 0.5, 1, 2 and 3). These figures also display previous results for $D_{\mathrm{G}}^0(\Gamma, N, \kappa)$ and $D_{\mathrm{E}}^0(\Gamma, N, \kappa)$ for 3D DPs obtained by Vieillefosse *et al.*,[25] Ohta & Hamaguchi,[16] Daligault,[17,26] Shakoori *et al.*,[18] Charan *et al.*,[53] Lu *et al.*,[60] Hartmann *et al.*,[11] Ghannad[49] and the experimental results of $D_{\mathrm{G}}^0$ of Strickler *et al.*,[33] respectively. Moreover, present 2D SC-DPs results of $D_{\mathrm{G}}^0(\Gamma, N, \kappa)$ and $D_{\mathrm{E}}^0(\Gamma, N, \kappa)$ obtained from EMD are analyzed, compared and discussed with those calculated from different numerical schemes such as LMD,[13–15] BMD[12,19] and MD.[31,61] It is observed that $D_{\mathrm{G}}$ and $D_{\mathrm{E}}$ in 3D DPs are similar at the same parameters, even for different system sizes. The reported EMD simulation data for $D_{\mathrm{G}}^0$ and $D_{\mathrm{E}}^0$ in 2D SC-DPs are higher than the previous MD data for $D_{\mathrm{G}}^0$ and $D_{\mathrm{E}}^0$ in 3D SC-DPs, in contrast with Vauilina *et al.*,[14] where their 2D data are lower than the 3D data. The possible reasons for this difference are the different normalizations, numerical approach, effective coupling, simulation time, etc.

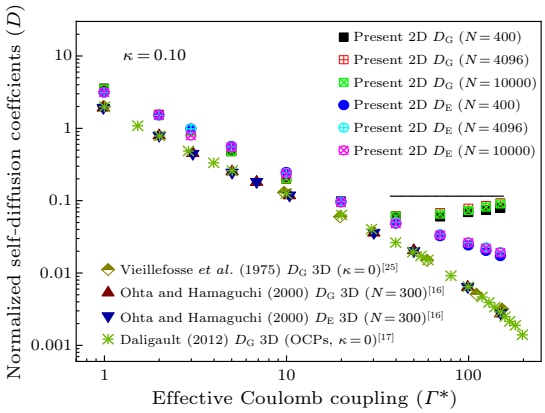



**Fig. 1.** Variations of normalized reduced $D^0_G(\Gamma^*, N, \kappa)$ and $D^0_E(\Gamma^*, N, \kappa)$ as a function of $\Gamma^*$ in 2D SC-DPs for $N = 400$, 4096 and 10000, respectively, at $\kappa = 0.10$. Present MD simulation outcomes are compared with earlier MD simulation data of 3D OCPs investigated by Vieillefosse *et al.*[25] ($D_G$), 3D SC-DPs of Ohta and Hamaguchi[16] ($D_G$, $D_E$) at $N = 300$ and 3D OCPs of Daligault[17] ($D_G$).

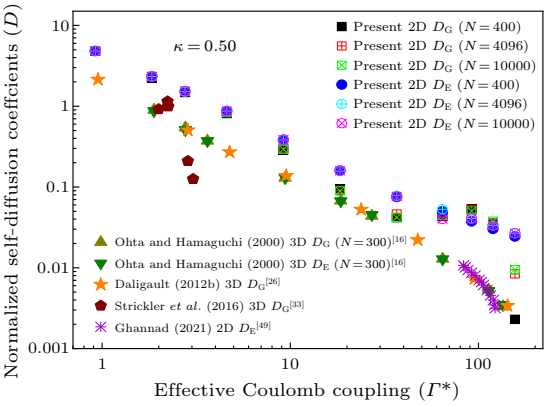



**Fig. 2.** Variations of normalized reduced $D^0_G(\Gamma^*, N, \kappa)$ and $D^0_E(\Gamma^*, N, \kappa)$ as a function of $\Gamma^*$ in 2D SC-DPs for $N = 400$, 4096 and 10000, respectively, at $\kappa = 0.50$. Present MD simulation outcomes are compared with earlier MD simulation data of 3D SC-DPs investigated by Ohta and Hamaguchi[16] ($D_G$, $D_E$) at $\kappa = 0.6$ and $N = 300$, Daligault[26] ($D_E$) at $N = 5000$–200 K, 3D experimental reported data of Strickler *et al.*[33] ($D_G$) and MD data of Ghannad[49] ($D_G$).

Figures 1 and 2 show the EMD outcomes of $D^0_G(\Gamma^*, N, \kappa)$ and $D^0_E(\Gamma^*, N, \kappa)$ for 2D SC-DPs as a function of $\Gamma^*$ at $\kappa = 0.10$ and 0.50, respectively, for three different system sizes ($N = 400$, 4096 and 10000). We have performed eleven different simulations at $\kappa = 0.1$ and 0.5 for each system size and a total of sixty-six to obtain data sets for comparison under the domain of plasma $\Gamma^*$. It should be noted that we rescale the $\Gamma$ parameter as an effective coupling ($\Gamma^*$) as proposed by Vaulina and Khrapak[62] for 3D DPs, where the $\Gamma^*$ is given as $\Gamma^* = \Gamma e^{-a\kappa}(1 - a\kappa + (a\kappa)^2/2)$. For 2D DPs, we follow the scaling suggested by Hartmann *et al.*,[63] which is suitable for infinite 2D systems. The effective coupling parameter in this case is $\Gamma^* = \Gamma(1 - 0.388\kappa^2 + 0.138\kappa^3 - 0.0138\kappa^4)$. The purpose of $\Gamma^*$ is to enable a further suitable comparison across systems of different dimensionality. The values of $D^0_G(\Gamma^*, N, \kappa)$ and $D^0_E(\Gamma^*, N, \kappa)$ linearly decreased with increasing the plasma coupling for the region of $0.97 \leq \Gamma^* \leq 39.5$ ($\kappa = 0.1$) and $0.92 \leq \Gamma^* \leq 36.78$ ($\kappa = 0.50$). It can be observed that the $D^0_G(\Gamma^*, N, \kappa)$ slightly increased for the region of plasma coupling $39.5 < \Gamma^* \leq 149.44$ ($\kappa = 0.10$) and slightly decreased for $64.36 \leq \Gamma^* \leq 149.44$ ($\kappa = 0.50$) but at $\Gamma^* = 156.30$ ($D^0_G$) again unexpectedly decreased. $D^0_E(\Gamma^*, N, \kappa)$ slightly deviate from their linear decreasing for $39.5 < \Gamma^* \leq 149.44$ ($\kappa = 0.10$) and slightly decreased $64.36 \leq \Gamma^* \leq 149.44$ ($\kappa = 0.50$). The data reported by Ghannad[49] and compared in Fig. 2, are significantly lower than present 2D results but match with 3D DP systems. The possible reason for this difference may be attributed to the different geometry of the simulation box, simulation time steps and run time. Figure 1 explains that for current MD data of $D^0_G(\Gamma^*, N, \kappa)$ and $D^0_E(\Gamma^*, N, \kappa)$ and data computed for 3D OCPs of Vieillefosse *et al.*,[25] Daligault computed from the same simulation scheme,[17,26] and $D_E$ at very small $\kappa = 0.10$ reported by Ohta and Hamaguchi[16] are the same. From Fig. 1, it can be concluded that no significant differences are observed in the previous literature at $\kappa = 0$ and $\kappa = 0.10$. EMD outcomes are also compared with 3D experimental estimation based on the G-K relation by Strickler *et al.*[33] for lower values of plasma coupling $\Gamma^*$ ($\approx$ 2–5). The experimental estimation is in fair agreement with EMD outcomes for 3D SC-DPs and lower than 2D EMD data in SC-DPs.

Three sets of plots (Figs. 3–5) are shown to explain the trends of computed plasma $D^0_G(\Gamma^*, N, \kappa)$ and $D^0_E(\Gamma^*, N, \kappa)$ in 2D SC-DPs at $\kappa = 1$, 2 and 3, respectively. Figures 3–5 (log-log scale) display the plasma $D^0_G$ and $D^0_E$ simulated through EMD simulations with varying $N = 400$, 4096 and 10000, respectively. For three cases, a different series of EMD simulations are performed as sixty for $\kappa = 1$, sixty-six ($\kappa = 2$) and ninety ($\kappa = 3$) for each system size. Both $D^0_G(\Gamma^*, N, \kappa)$ and $D^0_E(\Gamma^*, N, \kappa)$ are nearly the same and linearly decreased for the region $0.74 \leq \Gamma^* \leq 36.81$ ($\kappa = 1$), the same as for $0.33 \leq \Gamma^* \leq 16.56$ ($\kappa = 2$) and $0.12 \leq \Gamma^* \leq 11.62$ ($\kappa = 3$). The reported $D^0_G$ $(\Gamma^*, N, \kappa)$ remained nearly constant for the region $73.62 < \Gamma^* \leq 147.24$ ($\kappa = 1$), $33.12 < \Gamma^* \leq 132.47$ ($\kappa = 2$) and $23.24 < \Gamma^* \leq 127.82$ ($\kappa = 3$). However, $D^0_E(\Gamma^*, N, \kappa)$ decreased slightly for $73.62 < \Gamma^* \leq 147.24$ ($\kappa = 1$) and at $\kappa = 2$, and 3 linearly decreased for simulated range $\Gamma^*$, which agrees with experimental results.[10] It is noted that the well-matched region of $D^0(\Gamma^*, \kappa)$ increased with increasing the plasma density ($= \kappa$). The data obtained by Lu *et al.*[60] for 2D DPs is lower than the present 2D data and is well matched with 3D systems. The possible reason for this difference is the different approach (LMD), fractional drag coefficients ($\nu = 0.027\omega_p^{-1}$), different integration time steps $0.037\omega_p^{-1}$ and $N = 1024$ for such long simulation ($500 \leq \omega_p t \leq 3000$). The data reported by Charan *et al.*[53] at $\kappa = 2$, $\Gamma^* = 150$ lies between the present 2D and previous 3D SC-DPs.

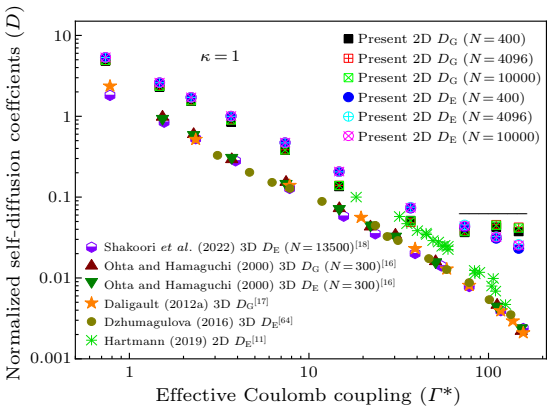



**Fig. 3.** Variations of $D_G^0(\Gamma^*, N, \kappa)$ and $D_E^0(\Gamma^*, N, \kappa)$ as a function of $\Gamma^*$ of 2D SC-DPs for $N = 400$, 4096 and 10000, respectively, at $\kappa = 1.0$. Present MD simulation outcomes are compared with earlier MD simulation data of 3D SC-DPs investigated by Shakoori *et al.*,[18] Ohta and Hamaguchi,[16] 3D OCPs of Daligault,[17] Dzhumagulova *et al.*[64] and Hartmann *et al.*[11]

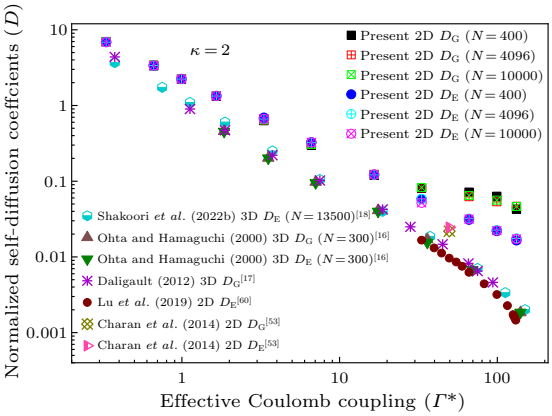



**Fig. 4.** Variations of $D_G^0(\Gamma^*, N, \kappa)$ and $D_E^0(\Gamma^*, N, \kappa)$ as a function of $\Gamma^*$ of 2D SC-DPs for $N = 400$, 4096 and 10000, respectively, at $\kappa = 2$. Present MD simulation outcomes are compared with earlier MD simulation data of 3D SC-DPs; see the caption of Fig. 2, as well as, Lu *et al.*[60] and Charan *et al.*[53]

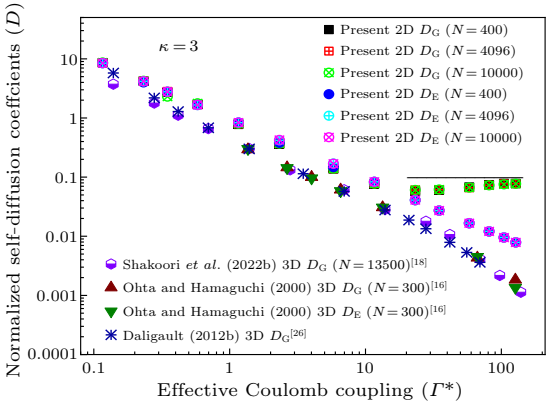



**Fig. 5.** Variations of $D_G^0(\Gamma^*, N, \kappa)$ and $D_E^0(\Gamma^*, N, \kappa)$ as a function of $\Gamma^*$ of 2D SC-DPs for $N = 400$, 4096 and 10000, respectively, at $\kappa = 3$. Present MD simulation outcomes are compared with earlier MD simulation data of 3D SC-DPs; see caption of Fig. 2.

In this study, EMD simulation was employed to investigate $D_G^0(\Gamma^*, N, \kappa)$ and $D_E^0(\Gamma^*, N, \kappa)$, which were obtained using the G-K and Einstein relations. We aim to assess the accuracy and applicability of the G-K and Einstein relations to $D_G^0$ and $D_E^0$ through EMD simulations in 2D DPs. These assessments have been made from two different perspectives; one is to check the validity of G-K and Einstein relations to produce diffusion coefficients, and the second is to determine the effects of varying system sizes on diffusion coefficients in 2D DPs.

It is observed that $D_G^0$ and $D_E^0$ are nearly the same for lower-to-intermediate values of $\Gamma$ (five times lower than the melting point $\Gamma_m$)[44] and different at higher $\Gamma$ values. The range of $\Gamma^*$ for these regions is different and significantly depends on $\kappa$, which can be clearly identified in Figs. 1–5. These results suggest that at low to intermediate $\Gamma^*$ values, the 2D DPs are in the warm liquid state, the system exhibits close to normal diffusion, and that is why both relations yield similar results, as suggested by Donko *et al.*[44] In the warm liquid state of DPs, the interparticle interactions are present but relatively weak compared to the thermal motion of dust particles. Due to the dominance of thermal fluctuation, the obtained diffusion coefficients are based on thermal energy. These results suggest that both relations accurately calculate the dynamics and interactions between dust particles at lower $\Gamma^*$ values.

The second region characterizes the divergence between $D_G^0$ and $D_E^0$. Specifically, $D_G^0$ at higher $\Gamma^*$ shows a slight increase for $\kappa = 0.1$ and 3.0 (see Figs. 1 and 5), a slight decrease for $\kappa = 0.5$ and 2.0 (see Figs. 2 and 4), and remains almost constant for $\kappa = 1.0$ (see Fig. 3). To check the consistency and validity of both $\Gamma^*$ and $D_G^0$, we replotted the values of $D_G^0$ at $N = 10000$, as shown in Fig. 6. We observed that for $\kappa = 0.1$–2.0, the $D_G^0$ data exhibited small variations, which are consistent. However, at $\kappa = 3.0$, the $D_G^0$ value was significantly lower, indicating inconsistency. The main reason for this inconsistency is that the equation for $\Gamma^*$ is only suitable for $\kappa = 0.1$–2.0, which agrees well with Ref. [63]. By combining all the data, we observe that $D_G^0$ decreases linearly over the small to intermediate range of $\Gamma^*$, while it shows slight variations for higher values of $\Gamma^*$. There are two possible reasons for this discrepancy. One is that the diffusion motion captured through VACF($t$) is not close to normal diffusion (anomalous) for the entire simulation time, see Fig. 7(a); thus, the $D_G^0$ data are not accurate. The other possible reason for the observed difference is that the VACF($t$) decays slowly in these regimes, due to stronger inter-particle interactions and more robust correlations between the dust particles [see Fig. 7(a)]. In this figure, we fit the decay of the VACF($t$) $\sim t^{\gamma}$ ($\gamma = -\mathrm{d}[\log(\mathrm{VACF}(t))]/\mathrm{d}[\log(t)]$), and observe that it follows a power law. The corresponding values of the decay exponent ($\gamma$) are displayed in Fig. 7(a), showing a slight increase in $\gamma$, which suggests a slight decrease in $D_G^0$ at higher $\Gamma^*$ values. Another possible reason is that the G-K relation does not accurately capture the inter-particle interactions and the microscopic dynamics of dust particles in these regimes.

This raises questions about the applicability and accuracy of the G-K relation in calculating diffusion in the cooled liquid states of 2D DPs. It can be argued that the G-K relation gives overestimations of $D_{\rm G}^0$, especially when compared to results obtained from the Einstein relation. This behavior may resemble the discrepancies observed in the calculation of shear viscosity.[65,66] Furthermore, $D_{\rm E}^0$ shows a slight decrease at lower $\kappa = 0.1$ to 1.0 and higher $\Gamma^*$. However, for $\kappa = 2$ and 3, $D_{\rm E}^0$ decreases almost linearly for computed $\Gamma^*$ values. These findings suggest that the accuracy of Einstein's relation improves as $\kappa$ increases. The transition from anomalous to normal diffusion (i.e., approaching normal diffusion) is observed over sufficiently long times. In this context, the Einstein relation ($D_{\rm E}^0$) may provide accurate results at higher $\Gamma^*$ values, indicating that the diffusive motion approaches normal diffusion (with $\alpha \approx 1$), particularly when the data is obtained over a long time ($\omega_{\rm p}t = 3000$), as shown in Fig. 7(b). This was further tested using MSD$(t) \sim t^{\alpha}(\alpha = {\rm d}[\log({\rm MSD}(t))]/{\rm d}[\log(t)])$ analysis, where at $\kappa = 2$ and for $\Gamma = 100$, 200, 300 and 396, the corresponding values of $\alpha$ were found to be 1.0865, 1.0783, 1.0323 and 1.0294, respectively. These values are in close agreement with the data reported in Ref. [60]. The values of $\alpha$ indicate that the diffusion is superdiffusive (anomalous), but approaches normal diffusion, which is consistent with the results in Ref. [60]; values of $0.98 \leq \alpha \leq 1.08$ were reported, with $\alpha \approx 1$. Overall, these results demonstrate that the Einstein relation provides more accurate diffusion coefficients compared to the G-K relation.

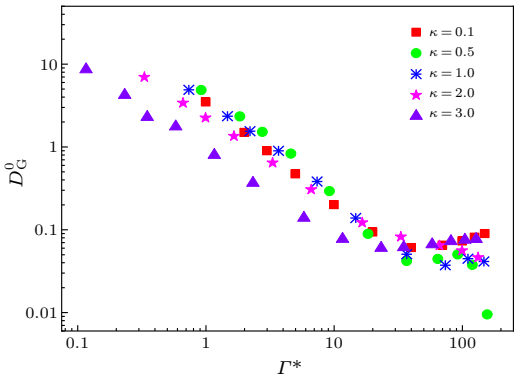



**Fig. 6.** Self-diffusion coefficients ($D_{\rm G}^0$) as a function of the effective coupling parameter ($\Gamma^*$) for five values of $\kappa = 0.1$, 0.5, 1.0, 2.0 and 3.0, and $N = 10000$.

Figures 1–5 demonstrate that $D_{\rm G}^0$ and $D_{\rm E}^0$ remain unaffected by system size when the plasma parameters are kept constant. This observation suggests that the diffusion coefficients are system size-independent. We explored this in more detail using both the G-K and Einstein relations. For the G-K relation, we calculated the VACF($t$) at $\Gamma = 100$ $\kappa = 2$ for different system sizes of $N = 400$, 1024, 4096 and 10000. The results, shown in the subgraph of Fig. 7(a), indicate that the VACF($t$) does not depend on the system size. The diffusion calculated through the Einstein relation in 2D DPs at sufficiently long times is independent of system size. A similar study was reported earlier in Ref. [41], where the authors observed that the MSD($t$) at long simulation times ($\omega_{\rm p}t = 3000$) showed that the diffusive motion approaches normal diffusion and is also independent of system size. We also performed a similar analysis by calculating MSD($t$) at a long simulation time ($\omega_{\rm p}t = 3000$) and fitting the curve. The results suggest that the diffusion motion tends towards normal diffusion, as shown in Fig. 7(b). Another possible factor influencing the system-size independence of diffusion coefficients could be the change in the geometry of the simulation box ($L_x \neq L_y$). While this might contribute to the observed results, it is still unclear which factors are dominant in ensuring that the diffusion coefficients remain system size-independent. In conclusion, our findings suggest that the diffusion coefficients in 2D DPs are system size-independent (true diffusion coefficients).

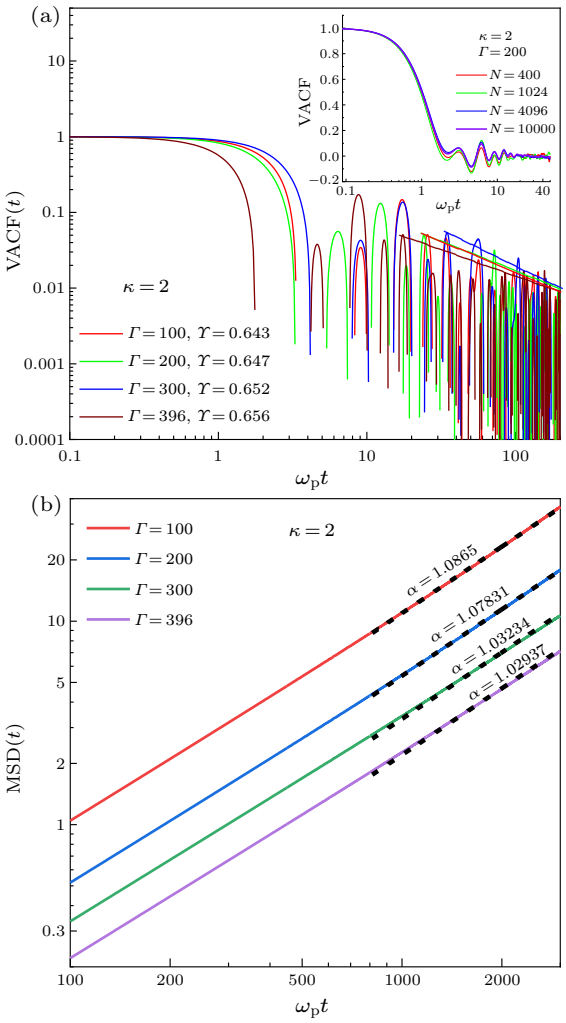



**Fig. 7.** Self-diffusion motion at $\Gamma = 100$, 200, 300 and 396 with $\kappa = 2.0$ (a) VACF (b) MSD($t$) as a function of time ($\omega_{\rm p}t$).

The EMD simulation outcomes of the self-diffusion coefficients are tested for simple temperature scaling law for

varying $N$ (= 400, 4096 and 10000) and are shown in Figs. 8 and 9. First, we normalized the diffusion coefficients ($D_{\rm G}$, $D_{\rm E}$) by Einstein frequency ($\omega_{\rm E}$) as $D^*_{\rm G} = D_{\rm G}/(\omega_{\rm E} a^2_{\rm ws})$ and $D^*_{\rm E} = D_{\rm E}/(\omega_{\rm E} a^2_{\rm ws})$[16–18] and the Einstein frequency is given as

$$\omega^2_{\rm E} = \frac{1}{2m}\sum_{i\neq j}\Delta\phi(\boldsymbol{r}_i - \boldsymbol{r}_j) = \frac{k^2_{\rm D}}{2m}\sum_{i\neq j}\phi(\boldsymbol{r}_i - \boldsymbol{r}_j). \quad (5)$$

These normalizations have already been used for 3D systems,[16–18,26] and are now implemented for 2D systems.[15] The simple temperature scaling law for the normalized self-diffusion coefficients can be written as

$$D^* = A(T^* - 1)^B + C, \quad (6)$$

where $A$, $B$ and $C$ are unknown fitting parameters, $T^*$ is the normalized temperature for 2D Yukawa systems, defined as $T^* = T/T_{\rm m} = \Gamma_{\rm m}/\Gamma$, $T_{\rm m}$ and $\Gamma_{\rm m}$ are the melting temperatures of liquid–solid critical point. The values of $\Gamma_{\rm m}$ are increased in magnitude with $\kappa$; the above relation is already used for 3D self-diffusion coefficients.[16,18,25] The simple temperature scaling law for fluid–solid transitions was explained in Ref. [13]. In this case, temperature scaling expression is implemented for the 2D SC-DPs $D^*_{\rm G}(T^*, \kappa, N)$ and $D^*_{\rm E}(T^*, \kappa, N)$ and are displayed in Figs. 8 and 9, respectively.

The temperature scaling law explains that $D^*_{\rm G}(T^*, \kappa, N)$ and $D^*_{\rm E}(T^*, \kappa, N)$ are plotted along the $y$-axis, while $T^*$ is plotted along the $x$-axis. The values of $D^*_{\rm G}(T^*, \kappa, N)$ and $D^*_{\rm E}(T^*, \kappa, N)$ are calculated for $N = 400$, 4096 and 10000 with five different values of $\kappa$ (= 0.1, 0.5, 1, 2 and 3). These diffusion coefficients are obtained through EMD simulations, capturing trends across various plasma phases, including gas-like, liquid-like and solid/crystal-like regimes. The dark lines (marked in red) in Figs. 8 and 9 represent the results obtained by applying the simple (universal) temperature scaling law functional form given in Eq. (6). The fitting Eq. (6) was used for the first time by Vieillefosse *et al.*,[25] followed by Ohta & Hamaguchi.[16] Then, there were different scaling approaches by Khrapak *et al.*[22] and most recently Shakoori *et al.*[18,27,28] for the 3D DPs. Implementing Eq. (6) yields appropriate fits to the normalized data of $D^*_{\rm G}(T^*, \kappa, N)$ and $D^*_{\rm E}(T^*, \kappa, N)$, from which unknown fitting parameters ($A$, $B$, $C$) are obtained. For $D^*_{\rm G}(T^*, \kappa, N)$, the fitting parameter values are found to be $A = 0.04138$, $B = 0.99572$ and $C = 0.0662$ for $N = 400$, $A = 0.01229$, $B = 1.21152$ and $C = 0.07909$ for $N = 4096$, and $A = 0.01228$, $B = 1.23566$ and $C = 0.09314$ for $N = 10000$. As $\kappa$ increases from 0.10 to 3, the values of Einstein frequency and $\Gamma_{\rm m}$ increase by more than an order of magnitude.[16] The variations in the fitting parameter values are relatively small when varying $N$. Figures 1–5 demonstrate that diffusion coefficients in 2D DPs are independent of system size, so here, parameter variations are very small. $D^*_{\rm G}(T^*, \kappa, N)$ does not accurately follow the temperature scaling law for the cold state of 2D SC-DPs ($0.8 \leq T^* \leq 10$). Our investigation demonstrates that the G-K relation is not valid in the cold liquid states of 2D DPs, because VACF indicates that diffusion motion is anomalous. However, in the gas–liquid or warm liquid states ($10 < T^* \leq 1000$), it accurately follows a linear trend, consistent with earlier literature.[18,27,28] This means that $D^*_{\rm G}$ deviates from the theoretical curves at low values of $\kappa$ and low temperature.

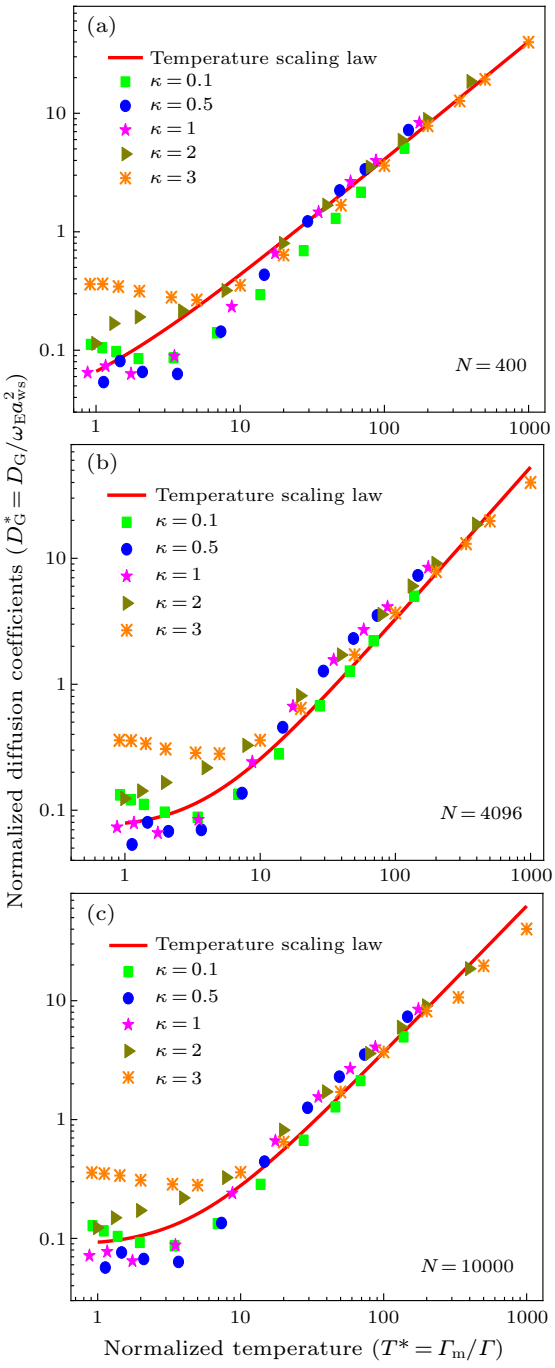



**Fig. 8.** Self-diffusion coefficients normalized by Einstein frequency [Eq. (5)] [$D^*_{\rm G}(T^*, \kappa, N)$] as a function of normalized temperature ($T^*$) for varying system size ($N = 400$, 4096 and 10000) at $\kappa = 0.10$, 0.50, 1, 2 and 3. Dark red line is derived from the universal temperature scaling law [Eq. (6)] for 2D SC-DPs. Present fitting curve of 2D DPs agrees with the previous 3D DP fitting curve reported by Ohta & Hamaguchi[16] and Shakoori *et al.*[18,27,28]

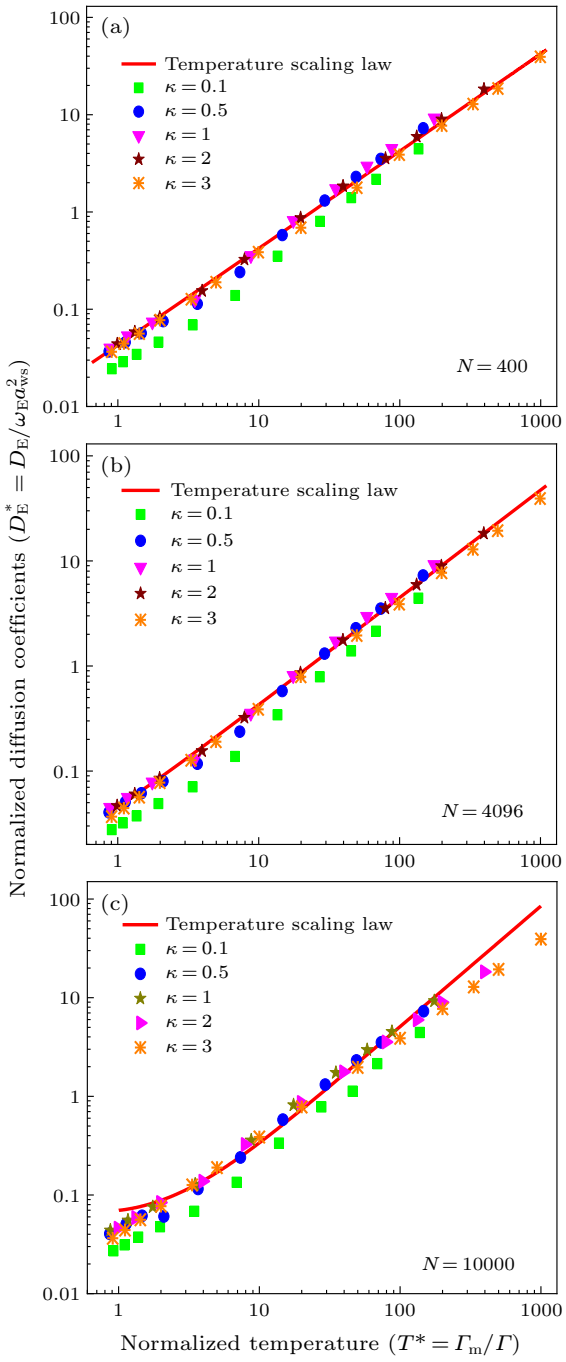



**Fig. 9.** Self-diffusion coefficients normalized by Einstein frequency [$D^*_E(T^*, \kappa, N)$] as a function of normalized temperature ($T^*$) for varying system size ($N$ = 400, 4096 and 10000) at $\kappa$ = 0.10, 0.50, 1, 2 and 3. Dark red line is derived from the simple temperature scaling law given in Eq. (6) for 2D SC-DPs. Present fitting curve of 2D DPs agrees with the previous fitting curve of 3D DPs reported by Ohta and Hamaguchi[16] and Shakoori *et al.*[18,27,28]

The fitting parameters for $D^*_E(T^*, \kappa, N)$ are $A = 0.04214$, $B = 1.0$ and $C = 0.04278$ for $N = 400$, $A = 0.04031$, $B = 1.02248$ and $C = 0.04639$ for $N = 4096$ and $A = 0.01823$, $B = 1.22264$ and $C = 0.06992$ for $N = 10000$. The fitting parameters are obtained after the fitting curve of the functional form given in Eq. (6) for both cases. The values of fitting parameters are close for different numbers of particles but different for the G-K and the Einstein relations. The $D^*_G(T^*, \kappa, N)$ and $D^*_G(T^*, \kappa, N)$ data lie around the red line, showing that the present EMD outcomes for 2D SC-DPs follow the simple temperature scaling law for the 3D system. It is significant that these fitting parameters propose that scaled $D^*$ is independent of $N$ and dependent on $\kappa$, validating the earlier simulation data.[18] It is analyzed from three panels that the computed data of $D^*$ are aligned along a dark line for a complete range of $\kappa$, except when very small (= 0.10), and the functional form gives an excellent fit. The functional form precisely produces the shape of the obtained $D^*$ curve, validating the earlier SC-DPs data[18] and giving an excellent relationship between $D^*$ and $T^*$ for a whole range of DP parameters ($\Gamma$, $\kappa$). Overall, the normalized Einstein diffusion coefficient mostly agrees with the theoretical curve at low temperatures and small Debye length.

## 4. Conclusion

In this paper, we investigate the self-diffusion coefficients in two-dimensional (2D) strongly coupled dusty plasma (SC-DP) liquids through equilibrium molecular dynamics simulations. The diffusion coefficients are computed through Green–Kubo ($D_G$) and Einstein ($D_E$) relations for a wide range of plasma screening ($\kappa$) and coupling ($\Gamma$) parameters. Simulations are performed for the three different system sizes, and outcomes are compared with previously available numerical and experimental data of 2D and three-dimensional SC-DPs. These investigations demonstrate that the different system sizes did not affect the values of $D_G$ and $D_E$. The Green–Kubo and Einstein relations provide nearly similar results for a small to intermediate range of plasmas $\Gamma$ (warm liquid states), depending on $\kappa$. However, for higher $\Gamma$ values, $D_G$ are overestimated because the VACF indicates the anomalous diffusion; thus, the $D_G$ are not accurate, while $D_E$ gradually decreases with increasing the $\Gamma$. Our chief findings indicate that the Einstein relation can provide accurate and valid diffusion coefficients over long timescales since diffusion motion tends to resemble normal diffusion.

## Data availability statement

The data that support the findings of this study are available from the corresponding authors upon reasonable request.

## Acknowledgements

Haipeng Li acknowledges the support of the Fundamental Research Funds for the Central Universities of China (Grant No. 2019ZDPY16). The authors thank the National Centre for Physics Islamabad, Pakistan, for allocating the High-Performance Computing platform and the Cluster for allocating computational power to check and run our MD code.

## References


[1] Ivlev A, Lowen H, Morfill G and Royall C P 2012 *Complex Plasmas and Colloidal Dispersions Particle-Resolved Studies of Classical Liquids and Solids* (Singapore: World Scientific)
[2] Grimes C C and Adams G 1979 *Rev. Lett.* **42** 795
[3] Gammel P L, Bishop G J, Kwo J R, *et al.* 1987 *Phys. Rev. Lett.* **59** 2592
[4] Murray C A, Sprenger W O and Wenk R A 1990 *Phys. Rev. B* **42** 688
[5] Mitchell T B, Bollinger J J, Huang X P, *et al.* 1999 *Phys. Plasmas* **6** 1751
[6] Fortov V E and Morfill G E 2009 *Complex and Dusty Plasmas* (CRC Press)
[7] Shakoori M A, Rahim I, Khan M, *et al.* 2024 *Phys. Scr.* **100** 2
[8] Dietrich K, Renggli D, Zanini M, *et al.* 2017 *New J. Phys.* **19** 065008
[9] Beckers J, Berndt J, Block D, *et al.* 2023 *Phys. Plasmas* **30** 120601
[10] Nunomura S, Samsonov D, Zhdanov S and Morfill G 2006 *Phys. Rev. Lett.* **96** 015003
[11] Hartmann P, Reyes J C, Kostadinova E G, *et al.* 2019 *Phys. Rev. E* **99** 013203
[12] Vaulina O S and Vladimirov S V 2002 *Phys. Plasmas* **9** 835
[13] Vaulina O S, Vladimirov S V, Petrov O F and Fortov V E 2004 *Phys. Plasmas* **11** 3234
[14] Vaulina O S and Dranzhevski I E 2006 *Phys. Scr.* **73** 577
[15] Vaulina O S, Adamovich X G, Petrov O F and Fortov V E 2008 *Phys. Rev. E* **77** 066403
[16] Ohta H and Hamaguchi S 2000 *Phys. Plasmas* **7** 4506
[17] Daligault J 2012 *Phys. Rev. Lett.* **108** 225004
[18] Shakoori M A, He M and Shahzad A 2022 *Eur. Phys. J. D* **76** 227
[19] Löwen H, Hansen J P and Roux J N 1991 *Phys. Rev. A* **44** 1169
[20] Baalrud S D and Daligault J 2013 *Phys. Rev. Lett.* **110** 235001
[21] Baalrud S D and Daligault J 2015 *Phys. Rev. E* **91** 063107
[22] Khrapak S A, Vaulina O S and Morfill G E 2012 *Phys. Plasmas* **19** 034503
[23] Rosenfeld Y, Nardi E and Zinamon Z 1995 *Phys. Rev. Lett.* **75** 2490
[24] Daligault J 2006 *Phys. Rev. Lett.* **96** 065003
[25] Vieillefosse P and Hansen J P 1975 *Phys. Rev. A* **12** 1106
[26] Daligault J 2012 *Phys. Rev. E* **86** 047401
[27] Shakoori M A, He M G, Shahzad A and Khan M 2022 *J. Mol. Model* **28** 398
[28] Shakoori M A, He M G, Shahzad A and Khan M 2022 *Plasma Phys. Reports* **48** 1023
[29] Shakoori M A, He M G, Shahzad A, Khan M and Zhang Y 2021 *Emerging Development and application of low temperature plasma* (IGI Global) p. 63
[30] Shakoori M A, He Maogang, Shahzad A and Khan M 2023 *Phys. Scr.* **98** 015608
[31] Begum M and Das N 2016 *IOSR Journal of Applied Physics* **8** 49
[32] Shakoori M A, He Maogang, Shahzad A, *et al.* 2022 *Studies of Self Diffusion Coefficient in Electrorheological Complex Plasmas through Molecular Dynamics Simulations* (Intech London)
[33] Strickler T S, Langin T K, McQuillen P, Daligault J and Killian T C 2016 *Phys. Rev. X* **6** 021021
[34] Robbins M O, Kremer K and Grest G S 1988 *J. Chem. Phys.* **88** 3286
[35] Rosenfeld Y, Nardi E and Zinamon Z 1995 *Phys. Rev. Lett.* **75** 2490
[36] Daligault J 2006 *Phys. Rev. Lett.* **96** 065003
[37] Liu Y, Liu B, Yang S Z and Wang L 2002 *J. Phys. A Math Gen* **35** 9535
[38] Liu B, Goree J and Vaulina O S 2006 *Phys. Rev. Lett.* **96** 015005
[39] Liu B and Goree J 2007 *S Phys. Rev. E* **75** 016405
[40] Liu B and Goree J 2008 *Phys Rev. Lett.* **100** 055003
[41] Liu B, Goree J and Feng Y 2008 *Phys. Rev. E* **78** 046403
[42] Liu B and Goree J 2014 *Phys. Plasmas* **21** 063704
[43] Hou L J, Piel A and Shukla P K 2009 *Phys. Rev. Lett.* **102** 085002
[44] Donkó Z, Goree J, Hartmann P and Liu B 2009 *Phys. Rev. E* **79** 026401
[45] Shahzad A and He M G 2012 *Phys. Scr.* **86** 015502
[46] Shahzad A, He M G and He K 2013 *Phys. Scr.* **87** 035501
[47] Ghannad Z and Hakimi Pajouh H 2017 *Phys. Lett. A* **381** 3952
[48] Ghannad Z 2019 *Phys. Rev. E* **100** 033211
[49] Ghannad Z 2021 *Phys. Plasmas.* **28** 043702
[50] Kostadinova E G, Banka R, Padgett J L, Liaw C D, Matthews L S and Hyde T W 2021 *Phys. Plasmas* **28** 073705
[51] Sheridan T E 2016 *Phys. Scr.* **91** 095603
[52] Wang H and Du J 2022 *Chinese Journal of Physics* **75** 169
[53] Charan H, Ganesh R and Joy A 2014 *J. Plasma Phys.* **80** 895
[54] Losseva T V, Popel S I, Yu M Y and Ma J X 2007 *Phys. Rev. E* **75** 046403
[55] Gabdulin A Z, Ramazanov T S and Moldabekov Z A 2017 *Contributions to Plasma Physics* **57** 458
[56] Rapaport D C 2002 *The art of molecular dynamics simulation* (Cambridge University Press)
[57] Busch J and Paschek D 2024 *J. Phys. Chem. B* **128** 1040
[58] Mazars M 2007 *J. Chem. Phys.* **126** 30
[59] Ott T and Bonitz M 2009 *Phys. Rev. Lett.* **103** 195001
[60] Lu S, Wang K and Feng Y 2019 *Phys. Plasmas* **26** 053704
[61] Begum M and Das N 2016 *Eur. Phys. J. Plus* **131** 1
[62] Vaulina O S and Khrapak S A 2000 *J. Exp. Theor. Phys.* **90** 287
[63] Hartmann P, Kalman G J, Donko Z and Kutasi K 2005 *Phys. Rev. E* **72** 026409
[64] Dzhumagulova K N, Masheyeva R U, Ott T, *et al.* *Phys. Rev. E* **93** 063209
[65] Haralson Z and Goree J 2017 *Phys. Rev. Lett.* **118** 195001
[66] Liu Y, Blosczy K N and Block D 2023 *Phys. Plasmas* **30** 043705